ARTICLE OPEN

Check for updates

Over-integration of visual network in major depressive disorder and its association with gene expression profiles

Mingrui Zhu[1,2,11], Yifan Chen[3,4,11], Junjie Zheng[4,5], Pengfei Zhao[4,5], Mingrui Xia[6,7,8]✉, Yanqing Tang[9]✉ and Fei Wang[2,4,5,10]✉

Major depressive disorder (MDD) is a common psychiatric condition associated with aberrant functional connectivity in large-scale brain networks. However, it is unclear how the network dysfunction is characterized by imbalance or derangement of network modular interaction in MDD patients and whether this disruption is associated with gene expression profiles. We included 262 MDD patients and 297 healthy controls, embarking on a comprehensive analysis of intrinsic brain activity using resting-state functional magnetic resonance imaging (R-fMRI). We assessed brain network integration by calculating the Participation Coefficient (PC) and conducted an analysis of intra- and inter-modular connections to reveal the dysconnectivity patterns underlying abnormal PC manifestations. Besides, we explored the potential relationship between the above graph theory measures and clinical symptoms severity in MDD. Finally, we sought to uncover the association between aberrant graph theory measures and postmortem gene expression data sourced from the Allen Human Brain Atlas (AHBA). Relative to the controls, alterations in systemic functional connectivity were observed in MDD patients. Specifically, increased PC within the bilateral visual network (VIS) was found, accompanied by elevated functional connectivities (FCs) between VIS and both higher-order networks and Limbic network (Limbic), contrasted by diminished FCs within the VIS and between the VIS and the sensorimotor network (SMN). The clinical correlations indicated positive associations between inter-VIS FCs and depression symptom, whereas negative correlations were noted between intra-VIS FCs with depression symptom and cognitive disfunction. The transcriptional profiles explained 21–23.5% variance of the altered brain network system dysconnectivity pattern, with the most correlated genes enriched in trans-synaptic signaling and ion transport regulation. These results highlight the modular connectome dysfunctions characteristic of MDD and its linkage with gene expression profiles and clinical symptomatology, providing insight into the neurobiological underpinnings and holding potential implications for clinical management and therapeutic interventions in MDD.

Translational Psychiatry (2025)15:86 ; https://doi.org/10.1038/s41398-025-03265-y

INTRODUCTION

Major depressive disorder (MDD) is one of the most common serious psychiatric disorders, characterized by persistent low mood, loss of interest and cognitive deficits, with a lifetime prevalence of up to 20 and 30% in men and women, respectively [1, 2]. Despite significant efforts, the pathophysiology of MDD remains poorly understood. However, MDD is increasingly recognized as a brain "dysconnectivity" disorder [3, 4]. Consequently, exploring the neurobiological underpinnings of MDD from a brain connectome perspective could offer a reasonable entry point and the development of new treatment targets for MDD.

Recent progress in integrating resting-state functional magnetic resonance imaging (R-fMRI) with connectome analysis has facilitated in vivo studies that have helped elucidate the inherent functional brain networks of humans [5–8]. Typically, the modular architecture of a healthy brain is characterized by an optimized network organization, which segregating the brain into various functional systems/modules with dense intramodular but sparse intermodular connections [8]. This modular network organization is pivotal for sustaining the balance between functional specialization and integration, thereby supporting emotional control and cognitive abilities [5–10]. However, convergent evidence from fMRI studies has shown that this balance is alerted in MDD, manifesting as aberrant intra- and inter- connectivity of specific functional systems encompassing both higher-order and primary networks [11–25]. Specifically, within each of these networks, substantial alterations in intra-modular connectivity have been consistently observed in patients with MDD. For instance, the default mode network (DMN), known for its role in self-referential thought processes, demonstrates significantly reduced functional connectivity within its subsystems, leading to abnormal

[1]Department of Neurology, Liaoning Provincial People's Hospital, Shenyang, Liaoning, China. [2]Department of Psychiatry, The First Affiliated Hospital of China Medical University, Shenyang, Liaoning, China. [3]School of Public Health, Southeast University, Nanjing, China. [4]Early Intervention Unit, Department of Psychiatry, The Affiliated Brain Hospital of Nanjing Medical University, Nanjing, China. [5]Functional Brain Imaging Institute of Nanjing Medical University, Nanjing, China. [6]State Key Laboratory of Cognitive Neuroscience and Learning, Beijing Normal University, Beijing, China. [7]Beijing Key Laboratory of Brain Imaging and Connectomics, Beijing Normal University, Beijing, China. [8]IDG/McGovern Institute for Brain Research, Beijing Normal University, Beijing, P. R. China. [9]Department of psychaitry, Shengjing Hospital of China Medical University, Shenyang, Liaoning, China. [10]Department of Mental Health, School of Public Health, Nanjing Medical University, Nanjing, China. [11]These authors contributed equally: Mingrui Zhu, Yifan Chen.
✉email: mxia@bnu.edu.cn; tangyanqing@cmu.edu.cn; fei.wang@yale.edu

Received: 15 March 2024 Revised: 6 January 2025 Accepted: 28 January 2025
Published online: 17 March 2025

rumination and pathological introspection [11–13]. In the frontoparietal network (FPN), which is crucial for cognitive control and executive functioning, decreased intra-network segregation has been observed, which contributes to the impaired executive function and cognitive control symptoms commonly reported in MDD [14–17]. Similarly, the salience network (SN), which is pivotal in identifying and responding to emotionally salient stimuli, exhibits reduced connectivity within key nodes such as the anterior insula and the dorsal anterior cingulate cortex. This deficiency is associated with a failure to properly detect and prioritize emotionally salient events, potentially exacerbating mood dysregulation and the persistence of negative affect [18–20]. Additionally, imbalanced inter-modular connections between distinct functional systems are implicated in various traits of MDD. For instance, cognitive models of MDD proposed that imbalanced connectivity between DMN, FPN and SN leads to impaired regulation of introspection, external attention, and mood [15, 21, 22]. In primary networks, dysconnectivity of the VIS and auditory network in MDD patients may lead to impaired facial processing, sound processing, and integration of visual and auditory information [23]. Furthermore, a resting-state fMRI study involving 56 MDD patients and 53 healthy controls (HCs) applied the participation coefficient (PC)-a modular architecture metric- to quantify inter- and intra-module connections of brain networks, finding that MDD participants had higher FPN integration and increased interconnections between the FPN, cingulo-opercular network, and cerebellum [14]. Another study found distinct modular architectures between MDD patients and HC, with increased PC in the left orbitofrontal cortex and paracentral lobule, decreased PC in the left superior parietal lobule, and abnormal integration between higher-order and primary functional systems involving the DMN, FPN, and sensorimotor network (SMN) in MDD [26]. These studies indicate that MDD is indeed a "dysconnectivity" disorder characterized by changes in the functional brain network modular. Due to the limited number of studies on modular architecture in MDD and their inconsistent findings, more research is needed to robustly identify of the neural alterations in MDD.

Moreover, much research has indicated that MDD is a moderately heritable disorder, with meta-analyses estimating its heritability to be 31–42% [27–29]. Genome-wide association studies (GWAS) have identified 44 risk variants linked to MDD, and which have been found to be linked to clinical symptoms of MDD, various anatomical brain regions [30, 31] and biological functions [31, 32]. Notably, genetic factors also play a crucial role in the brain connectome organization [33]. Recently, transcriptome-connectome association studies have emerged, offering an unprecedented capacity to bridge the gap between the microscale transcriptome profile and the macroscale brain network [34–37]. Specifically, the organization of intrinsic functional brain network systems has been associated with gene co-expression patterns in the brain, with these genes primarily involved in ion channel activity, oxidative metabolism, and synaptic-related functions [32, 35, 38]. More recently, by linking ex vivo transcriptome data with the in vivo gradient structure of functional brain networks in MDD patients, Xia et al. identified genes associated with gradient changes in MDD, with the most correlated genes enriched in transsynaptic signaling and calcium ion binding [32]. Therefore, if MDD patients present alterations in the macroscale functional organization of brain modules, we speculate that connectome dysfunction in brain networks may potentially be associated with specific transcriptome profiles. Clarifying this link could deepen our insight into molecular genetic underpinnings of connectome dysfunction of brain network system in MDD.

In this study, we integrated an R-fMRI dataset of 559 individuals with transcriptomic data from the brains of six donors provided by the Allen Human Brain Atlas (AHBA) from the Allen Institute for Brain Science (AIBS) [34, 39], to investigate the modular connectome patterns of brain networks in MDD and their relationships with gene expression profiles. Firstly, we identified MDD-related connectome dysfunction in brain network system by computing PC and further intra- and inter-modular connections. Secondly, we established the relationship between the above graph theory measures and the severity of clinical symptoms in MDD. Finally, we used AHBA to identify genes spatially correlated with the modular connectome pattern of MDD and preformed enrichment analysis for biological pathways related to the modular connectome in brain network system of MDD.

MATERIALS AND METHODS

Participants

We recruited 262 patients with MDD and 297 healthy controls (HC), aged 18–45 years. The patients with MDD were recruited from the inpatient department of the Shenyang Mental Health Center and the outpatient clinic of the Department of Psychiatry of the First Affiliated Hospital of China Medical University in Shenyang, China. The study received approval from the ethics committees of China Medical University, and every participant provided written informed consent. For details about all participants'diagnostic procedures, demographic and clinical information, see Supplementary Materials.

Image acquisition and MRI processing

Information on the R-fMRI scan parameters and participants requirements during scan is detailed in Supplementary Materials. All R-fMRI images were preprocessed using GRETNA toolbox [40] following a specific pipeline. In summary, the initial steps in preprocessing involved converting DICOM files to nifti format, discarding the initial 10 volumes for signal stabilization, and then proceeding with slice-timing and head motion corrections, excluding any subject movement beyond 3 mm or 3°. Spatial normalization was carried out to align with the Montreal Neurological Institute space using an echo-planar imaging template, and images were resampled to 3-mm cubic voxels. Spatial smoothing was applied using a 4-mm full-width half-maximum Gaussian kernel. The preprocessing routine also included linear detrending and the regression of several nuisance variables, including Friston's 24 motion parameters, signals from white matter and cerebrospinal fluid, as well as the global signal. Temporal filtering was applied within the frequency range of 0.01 to 0.08 Hz. Frame-wise displacement exceeding 0.5 was addressed by scrubbing affected volumes, including one preceding and two subsequent volumes, with linear interpolation to mitigate the effects of head motion artifacts.

Network construction

Functional connectivity networks for each individual were constructed using nodes defined by the Human Connectome Project (HCP) atlas [41]. Pearson's correlation coefficient was calculated for each pair of nodes, resulting in a 360×360 correlation matrix for each participant. These matrices were then weighted using a default density threshold across a set of densities ranging from 0.05 to 0.5 (with an interval of 0.05), ensuring consistent edge counts across all network graphs [40, 42, 43]. see Supplementary Materials.

Module parcellation

Using the Yeo 7 network framework [44], we segmented the entire brain's functional networks into seven distinct modules, including the DMN,FPN, Dorsolateral Attention Network (DAN), Ventral Attention Network (VAN), Limbic Network (Limbic), VIS and SMN. Module detection was performed utilizing the PAGANI toolkit (www.nitrc.org/projects/pagani_toolkit/) [45].

Graph theory parameters calculation

The Participation Coefficient (PC) is an effective approach for calculating modular integration among brain networks [46]. The calculation of PC is based on the modular partitions of each subject's brain network. For each node within a subject's brain network, the PC is calculated using the following equation:

$$PC_i = 1 - \sum_{s=1}^{m} \left(\frac{kis}{ki}\right)^2$$

Where, for each given node i within module m, kis represents the number of links between node i and other nodes in module m, while ki represents the total connections node i has. The PC values for each individual were subsequently normalized as follows:

$$PC_{norm=}\frac{PC}{(N_{mod}-1)/_{N_{mod}}}$$

where Nmod is the number of modules per subject. Nodes were classified as connectors if their PC exceeded 0.3 [47]. Connectors play a crucial role associated with module integrity. Furthermore, using regions with significant group differences in PC as seeds, we detected functional connectivities (FCs) at both region-to-module and region-to-region levels throughout the brain, to explore how connections between different modules and regions contribute to group variances in PC, see Supplementary Materials.

Gene expression dataset and preprocessing

Gene expression data, derived from microarrays, were obtained from the AHBA [34, 39]. Tissue samples in the dataset came from the brains of six adult donors (average age: 42.5 years, including 1 female, detailed in Table S1). The gene expression microarray data were preprocessed using an established pipeline, which involved aligning the samples to a cortical parcellation consisting of 360 regions [41], reannotating and selecting probes, and normalizing data across donors [48], see Supplementary Material.

Statistical analysis

Demographic and clinical data. Independent two-sample *t*-tests (Gaussian distribution) or Mann Whitney U tests (No Gaussian distribution) were employed to investigate differences in age, education, MeanFD and clinical variables; the chi-square tests was employed in gender between the two groups. The threshold for significance level was defined as $P < 0.05$.

PC and FCs analysis. Taking age, gender, education and meanFD as covariates, the two sample *t*-test in each module was conducted for the PC between the two groups. The false discovery rate (FDR) correction was performed for multiple comparisons, and the significance was set to a corrected $P_{FDR} < 0.05$. After the FCs in region-to-module and FCs in region-to-region were calculated in two groups, taking age, gender, education, and mean FD as covariates, the two sample *t*-test was conducted for the two-level FCs respectively, $P_{FDR} < 0.05$.

Association analysis between clinical variables and MDD-related connectome measures (PC and FCs) alterations

Controlling age, gender, education and meanFD, we performed partial correlations analysis between connectome measures (MDD-related PC, MDD-related FCs in region-to-module and MDD-related FCs in region-to-region) and clinical variables(i.e., HAMD total and factors scores, MCCB and illness duration). For each brain connectome measures, FDR correction was performed between clinical variables, and the statistical difference was set to $P_{FDR} < 0.05$.

Association analysis between gene expression and MDD-related PC. We employed Partial Least Squares regression analysis [49] to investigate the relationship between transcriptional profiles and the PC map of between-group differences. Initially, we aligned the gene expression data (comprising 10,027 genes) with the between-group difference T-map of the PC, utilizing the Glasser 360 atlas [41]. In our PLS regression analysis, we designated the gene expression data as predictor variables and the T-map representing between-group PC differences as the response variable. For each PLS model, we implemented a permutation test, adjusted for spatial autocorrelation, to assess if the R2 value of the PLS component significantly exceeded chance levels. Subsequently, for every significant component, we applied a bootstrapping technique to adjust for estimation errors in the gene weights [50]. We sorted the genes based on their adjusted weights, indicating their significance to the PLS regression component, arranging them in descending order from the most positively to the most negatively associated. Genes with an absolute corrected weight above 5 were selected for a list of significantly contributing genes. This list was then subjected to enrichment analysis to identify prevalent Gene Ontology (GO) terms, utilizing a GO enrichment analysis and visualization tool (Metascope, https://metascape.org/) [51]. We considered all three ontology categories: biological process, cellular component, and molecular function, in addition to the KEGG pathway. Enrichment was deemed significant if it met a threshold set by a Benjamini-Hochberg FDR-corrected $q < 0.01$, see Supplementary Materials.

Validation analysis. To assess the potential impact of medication status and patient episodes on functional brain networks, we conducted the following analysis: First, patients were divided into subgroups based on their clinical information: medication vs. nonmedication subgroups and first episode vs. relapsed subgroups. Second, we conducted two-sample t-tests between each subgroup pair, analyzing both PC and FCs at two levels. Third, to ascertain the stability of gene expression and its pathways linked to MDD-related PC, we conducted a correlation analysis of gene expression from the perspective of whole-brain connectivity. Last, we also validated the influence of sex and hemisphere differences on this connectome-transcriptome association, see Supplementary Materials.

RESULTS

Demographic and clinical data

No significant differences in age, gender education level or MeanFD were observed between the MDD and HC groups (all $P > 0$ .05). In contrast, significant differences were observed in HAMD total score and factors scores, MCCB scores between groups. The detailed demographic and clinical data of the participants are summarized in Table S2.

Alterations in systemic function connection in MDD

PC. A significant group effect on PC was first observed in twelve brain regions. Notably, the twelve brain regions were primarily located in the bilateral visual network (VIS) ($P_{FDR} < 0.05$, Table 1, Fig. 1), specifically in the right primary visual cortex(V1), bilateral early visual cortex(V2 and V3), left dorsal stream visual cortex(V3A), bilateral ventral stream visual cortex(VMV1, VMV2 and VMV3), right posterior cingulate cortex(Pros) and the right medial temporal cortex(PHA1). No brain regions with PC differences between groups were found in other modules.

FCs in region-to-module. Taking the twelve regions within VIS that showed significant PC group effects as seeds, we established FCs between each of these regions and each of the seven modules to determine the contributions of different module connections to group differences in PC. Compared to HC group, MDD group have following significant differences: (1) High FCs inter VIS-High Order Network: the FC values between some VIS regions showing PC group effects and high order network (VIS-DMN, VIS-FPN, VIS-VAN) were increased, $P_{FDR} < 0.05$; (2) High FCs inter VIS-Limbic: the FC values between some VIS regions showing PC group effects and Limbic were increased, $P_{FDR} < 0.05$; (3) Low FCs intra-VIS: the FC values between some VIS regions showing PC group effects and the VIS were decreased, $P_{FDR} < 0.05$); Low FCs inter VIS-SMN: the FC values between some VIS regions showing PC group effects and SMN were decreased, $P_{FDR} < 0.05$), Fig. 2A–C and Table S3.

FCs in region-to-region. Taking the twelve regions within VIS that showed significant PC group effects as seeds, we established FCs between each of these regions and all regions across the whole brain to determine the contributions of different regional connections to group differences in PC. Compared to HC group, ninety-six FCs at region-level showed statistical differences in MDD, $P_{FDR} < 0.05$. The alterations of FCs at region-level align closely with the changes at module-level FCs in MDD: high FCs inter VIS and low FCs intra VIS, $P_{FDR} < 0.05$, see Fig. 2A, B, D and Tables S4, 5.

Relationship between graph theory parameters (PC and FCs) and clinical variables in MDD

No correlation was observed between MDD-related PCs and clinical variables. At the region-to-module level, negative

Table 1. Significant between MDD and HC group difference in PC ($P_{FDR} < 0.05$).

Modular/System	RoiID	Regions	Description (Glasser 360 atlas)	Cortex	T values	P values corrected
VIS	4	lh_V2	Second Visual Area L	Early Visual Cortex	3.19	0.0015
VIS	5	lh_V3	Third Visual Area L	Early Visual Cortex	3.14	0.0018
VIS	13	lh_V3A	Area V3A L	Dorsal Stream Visual Cortex	2.82	0.0050
VIS	154	lh_VMV3	VentroMedial Visual Area 3 L	Ventral Stream Visual Cortex	3.05	0.0024
VIS	160	lh_VMV2	VentroMedial Visual Area 2 L	Ventral Stream Visual Cortex	3.06	0.0024
VIS	181	rh_V1	Primary Visual Cortex R	Primary Visual Cortex	2.76	0.0060
VIS	185	rh_V3	Third Visual Area L	Early Visual Cortex	2.65	0.0107
VIS	301	rh_ProS	ProStriate Area R	Posterior Cingulate Cortex	2.80	0.0053
VIS	306	rh_PHA1	ParaHippocampal Area 1 R	Medial Temporal Cortex	3.37	0.0008
VIS	333	rh_VMV1	VentroMedial Visual Area 1 R	Ventral Stream Visual Cortex	3.23	0.0013
VIS	334	rh_VMV3	VentroMedial Visual Area 3 R	Ventral Stream Visual Cortex	2.65	0.0083
VIS	340	rh_VMV2	VentroMedial Visual Area 2 R	Ventral Stream Visual Cortex	2.84	0.0046

A significant group effect on PC located in twelve brain regions within bilateral VIS, PFDR < 0.05. They were the right primary visual cortex (V1), bilateral early visual cortex (V2 and V3), left dorsal stream visual cortex (V3A), bilateral ventral stream visual cortex (VMV1, VMV2 and VMV3), right posterior cingulate cortex (Pros) and the right medial temporal cortex (PHA1). VIS: Visual Network; RoiID: region number in Glasser 360 atlas; lh, L: left hemisphere; rh, R: right hemisphere.

VIS visual network, *RoiID* region number in glasser 360 atlas; lh, *L* left hemisphere; rh, *R* right hemisphere.

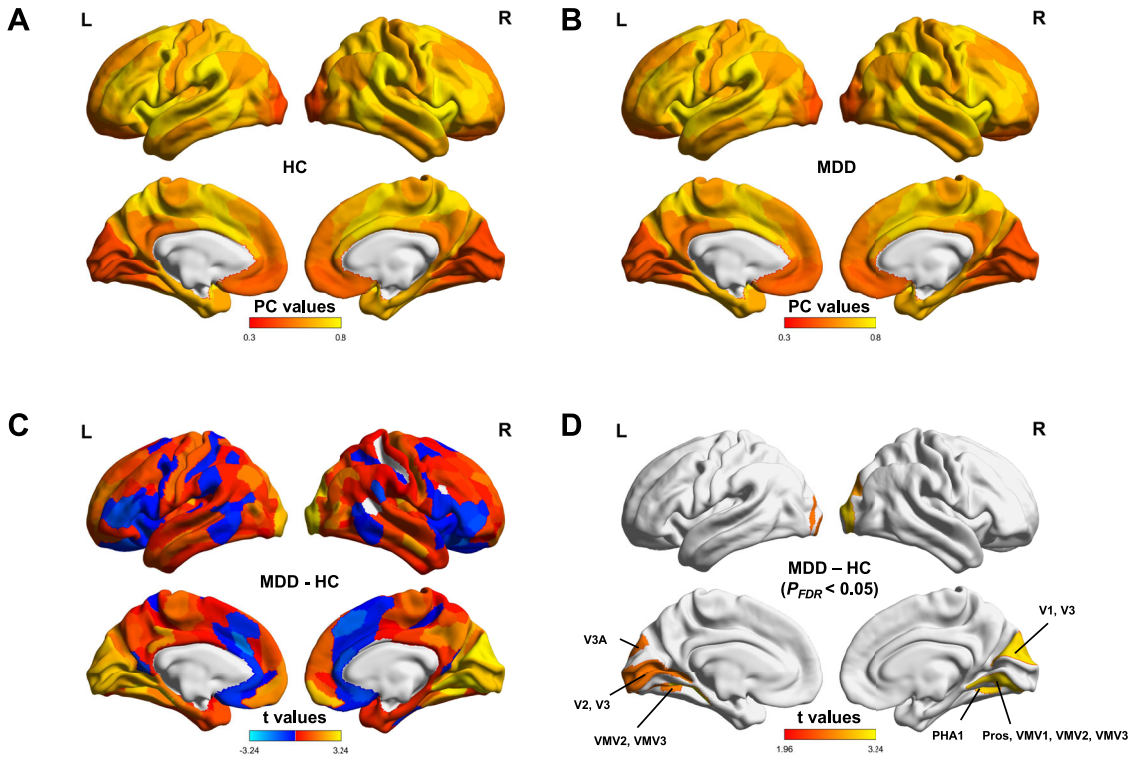

Fig. 1 Altered Patterns of PC in MDD. A Mean PC map for the HC group. **B** Mean PC map for the MDD group. **C** *t*-test map showing differences in PC between the MDD and HC groups (MDD vs. HC). **D** Group effects map showing significant differences in PC between the two groups (MDD vs. HC), $P_{FDR} < 0.05$. Significant regions include the right primary visual cortex (V1), bilateral early visual cortex (V2, V3), left dorsal stream visual cortex (V3A), bilateral ventral stream visual cortex (VMV1, VMV2, VMV3), posterior cingulate cortex (Pros), and the right medial temporal cortex (PHA1). PC: participation coefficient; MDD: major depressive disorder; HC: healthy control. The surface visualization was generated using BrainNet Viewer (http://www.nitrc.org/projects/bnv) [93].

correlations between the FC value of lh_VMV2-VIS and HAMD (total score, Core depressive Factor, Somatic anxiety Factor and Anorexia Factor scores, PFDR < 0.05) were found. No correlation was observed between MDD-related FCs in region-to-module level with MCCB and duration. However, at the region-to-region level, we did find significant negative correlations between a great number of intra-VIS FCs and HAMD (total and factors score, PFDR < 0.05), and positive correlations between regions of VIS-DMN with HAMD (total and factors score, PFDR < 0.05). We also observed significant positive correlations between intra-VIS (lh_V2- lh_ProS, and lh_V2-lh_VMV1) and Category Fluency in MCCB, $P_{FDR} < 0.05$. There was no significant correlation between

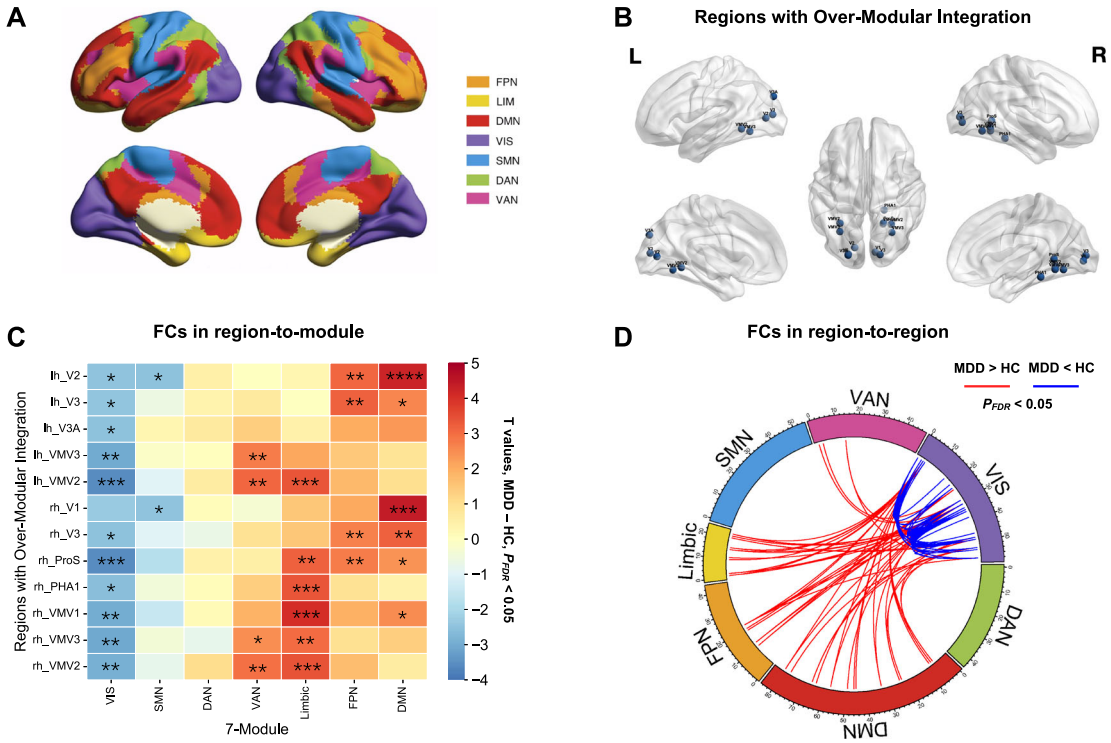

Fig. 2 Altered Patterns of FCs in MDD. A Seven-module brain network parcellation used for the analysis, derived from Yeo et al. [44]. These modules include the FPN, DMN, DAN, VAN, Limbic, VIS, and SMN. **B** Schematic representation of brain regions exhibiting significant group differences in PC between the MDD and HC groups. These regions, where modular integration is altered in MDD (see Fig 1D), are primarily located within the VIS ($P_{FDR} < 0.05$). These regions are the right primary visual cortex (V1), bilateral early visual cortex (V2, V3), left dorsal stream visual cortex (V3A), bilateral ventral stream visual cortex (VMV1, VMV2, VMV3), posterior cingulate cortex (Pros), and the right medial temporal cortex (PHA1). **C** Group differences in FCs at the region-to-module level. The FCs between each region with over-modular integration and each of the seven brain modules were established. Red areas indicate increased FCs in MDD compared to HC, while blue areas indicate decreased FCs in MDD. The significance of group differences is marked with asterisks: * $P_{FDR} < 0.05$, ** $P_{FDR} < 0.01$, *** $P_{FDR} < 0.001$, and **** $P_{FDR} < 0.0001$. **D** Group differences in FCs at the region-to-region level. Blue lines indicate significantly decreased FCs in MDD compared to HC, while red lines indicate significantly increased FCs in MDD compared to HC ($P_{FDR} < 0.05$). FCs: functional connectivities; MDD: major depressive disorder; HC: healthy control; FPN: frontoparietal network; DMN: default mode network; DAN: dorsolateral attention network, VAN: ventral attention network, Limbic: limbic network, VIS: visual network, and sensorimotor network (SMN).

FCs in regions-to region level and duration of disease. see Tables S6–8.

Gene expression profiles related to connectome dysfunction of brain network system in MDD

MDD-related alterations in PC and gene. The components of the PLS1 regression explained 21.0% of the variance in the MDD-related alterations in PC ($P < 0.05$ for component 1, permutation tests with spatial autocorrelation corrected, Fig. 3A). Component 1 represented a transcriptional profile characterized by high expression mainly in VIS areas (Fig. 3D). The spatial expression value weight of the gene corresponding to this component has a significant spatial positive correlation with the PC abnormal pattern of MDD (Fig. 3C) ($r = 0.46$, $P < 0.0001$), Fig. 3B. The PLS1 gene list is sorted according to the weight from large to small (Fig. 3E), and the genes with the absolute value of gene weight greater than 5 [52] are selected as the most significant gene list for the next analysis of biological pathways.

According to GO database, the GO functional terms with the most significant expression of PLS1 gene related to PC abnormal pattern of MDD are as follows. Figure 4A: biological process (BP) mainly includes "cross synaptic signal", "regulation of ion transport", "secretion regulation", etc; Cellular component (CC) mainly includes: "axon", "postsynaptic (membrane)" and "glutamatergic synapse"; Molecular function (MF) mainly includes "kinase binding" and "protein homodimerization activity". The KEGG functional pathway of PLS1 gene expression related to the PC abnormal pattern of MDD, corrected by FDR, has 12 KEGG pathways when $q < 0.01$, as shown in Fig. 4B: the main enrichment pathways are "cancer pathway", "glutamatergic synapse" and "RAS signal pathway".

Validation results

There is no difference among subgroups of drug treatment status and disease onset in each brain graph theory parameter (twelve of MDD-related PC, thirty-three of MDD-related FCs in region-to-module level, ninety-six of MDD-related FCs in region-to-region level, $P < 0.05$ see Tables S9–14. The gene expression and their pathways related to MDD-related FCs region-to region level were highly consistent with those of MDD-related alterations in PC, Figs. S1–2. Using gene data from male donors and gene data from the left hemisphere highly overlaps with the gene expression and biological pathways identified in our main results, Tables S15, 16.

DISCUSSION

In this study, we utilized the Participation Coefficient metric to explore the connectome dysfunction of brain functional network system of MDD patients and, for the first time, linked these atypical patterns with transcriptomic profiles. Alterations in systemic functional connectivity were observed in MDD. Specifically, compared to the HC group, the MDD group exhibited hyper-integrated network nodes, all located within the bilateral VIS. Further analysis of intra- and inter-modular connectivity at both

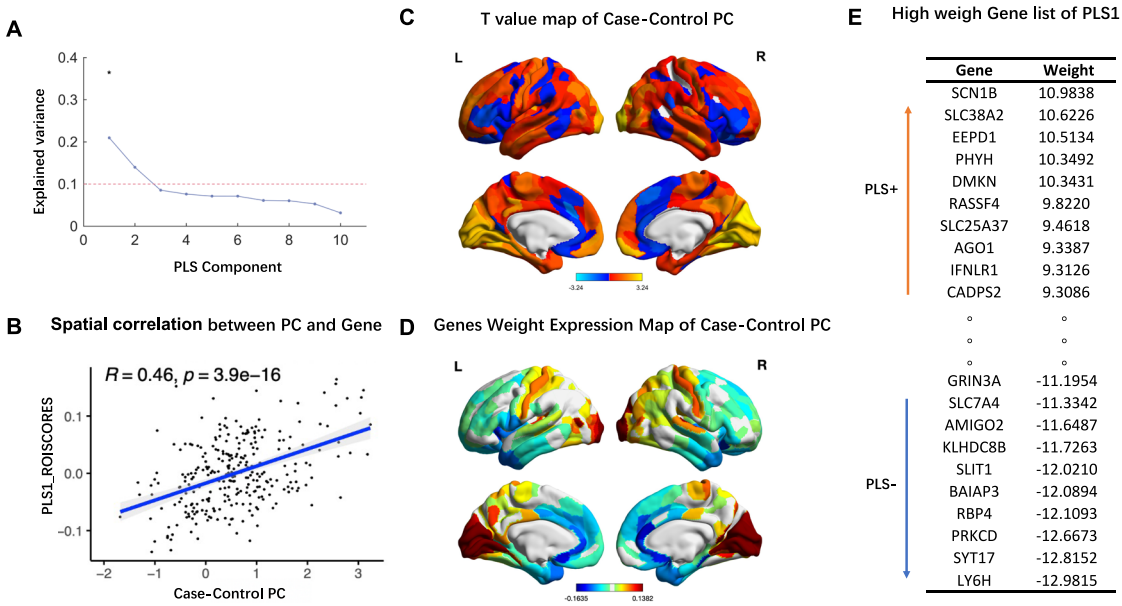

Gene	Weight
SCN1B	10.9838
SLC38A2	10.6226
EEPD1	10.5134
PHYH	10.3492
DMKN	10.3431
RASSF4	9.8220
SLC25A37	9.4618
AGO1	9.3387
IFNLR1	9.3126
CADPS2	9.3086
◦	◦
◦	◦
◦	◦
GRIN3A	-11.1954
SLC7A4	-11.3342
AMIGO2	-11.6487
KLHDC8B	-11.7263
SLIT1	-12.0210
BAIAP3	-12.0894
RBP4	-12.1093
PRKCD	-12.6673
SYT17	-12.8152
LY6H	-12.9815

Fig. 3 Imaging transcriptomics analysis of MDD-related PC. A Percentage of variance in effect variables explained by component decomposition of partial least squares regression analysis. The significance level was determined by the displacement test after spatial autocorrelation (n = 10000), * P < 0.05. The transcriptional profiles explained 21% variance of the altered PC pattern. The shadow indicates the 95% confidence intervals. Each dot represents a region. **B** Spatial correlation between PLS1 gene expression pattern and abnormal PC pattern of MDD visual network. The transcriptional profiles were positively correlated with the between-group Z-map of the PC (permutation tests with spatial autocorrelation corrected, 10,000 times). The shadow indicates the 5% confidence intervals. Each dot represents a region. **C** MDD visual network abnormal PC (T-value map of case-control PC). **D** The gene weight expression map obtained by PLS regression analysis (PLS1 weight Z map). The first PLS component (PLS 1) identified a gene expression profile with high expression mainly in VIS. VIS: Visual Network. *P < 0.05. **E** In the gene list sorted by PLS1, pls + represents the high expression gene with positive weight direction, and pls - represents the low expression gene with negative weight direction.

region-to-module and region-to-region levels revealed that the VIS had higher FC values with both higher-order networks (DMN, FPN, and VAN) and the LIM, but lower FC values within the VIS and between VIS and the primary SMN. Moreover, the clinical correlations indicated possive associations between inter-VIS FCs and HAMD scores, whereas negative correlations were noted between inter-VIS FCs with HAMD scores and Category Fluency score of MCCB. The transcriptional profiles explained 21–23.5% of the variance brain network system dysconnectivity pattern, with the most correlated genes enriched in trans-synaptic signaling and ion transport regulation. Our research provides profound insights into the connectome dysfunction in brain functional network system associated with MDD. The observed over-integration of VIS in MDD, its association with clinical symptoms severity, and its linkage to specific gene expression profiles provide a groundbreaking perspective on the underlying mechanisms of MDD.

Higher nodal integration of VIS

Through the analysis of the PC based on brain network functional systems, we identified a significant characteristic of MDD: higher nodal integration within the VIS, indicative of reorganization within this network. Specifically, these over-integrated nodes were located in the primary visual cortex (right V1), the early visual cortex (left V2 and bilateral V3), ventral stream visual cortex (right VMV1 and bilateral VMV2 and VMV3), the medial temporal cortex (right PHA 1) and the posterior cingulate cortex (right ProS). Functionally, V1, V2, and V3 play an important role in the bottom-up processing of visual information from the lateral geniculate nucleus, which is essential for visual perception [53, 54]. These areas can also encode specific visual information in the presence or absence of visual stimuli, thereby facilitating top-down visual processing and multisensory integration, both of which are essential for visual cognition [53, 54]. The VMV is implicated in emotion-related information processing and is closely linked to the pathophysiology of MDD [55]. The ProS is strongly connected to V2 and V3, and it has been found to be activated during working memory tasks [41]. The PHA1 is associated with visual memory tasks and plays a role in visual cognitive functions [41]. Previous studies have reported structural and functional abnormalities in these brain regions in MDD [24, 56–64]. Yang et al. have identified decreased nodal degrees and nodal efficiency within the VIS in MDD patients at the nodal level [62], which consistent with our finding. However, contrary to our findings, Peng et al. reported abnormalities in brain region integration within the DMN and FPN, but not in the VIS, among MDD patients [26]. Such discrepancies might be attributed to factors including sample size, disease state, and other related variables. Although our study utilized the relatively larger sample size among existing studies on modular integration of MDD, future research should include more participants to replicate and validate these results. In summary, our finding offers a novel perspective by identifying over-integration of key nodes within the VIS from a functional modular standpoint, adding fresh insights into the role of the VIS to the pathophysiology of MDD.

Abnormal system functioning connectome mode behind high VIS nodal integration

Further analysis detected that the higher modular integration of the VIS in MDD was driven by increased inter-VIS connections involving VIS-higher-order networks (DMN, FPN and VAN) and VIS-Limbic connections, alongside decreased intra- VIS connections. We also observed reduced inter-primary network connections between the VIS and SMN in MDD. Taken together, these findings illustrate an MDD related-abnormal system functioning connectome mode underlying high VIS nodal integration, providing new insights into how specific modular changes contribute to the whole brain network dysconnectivity.

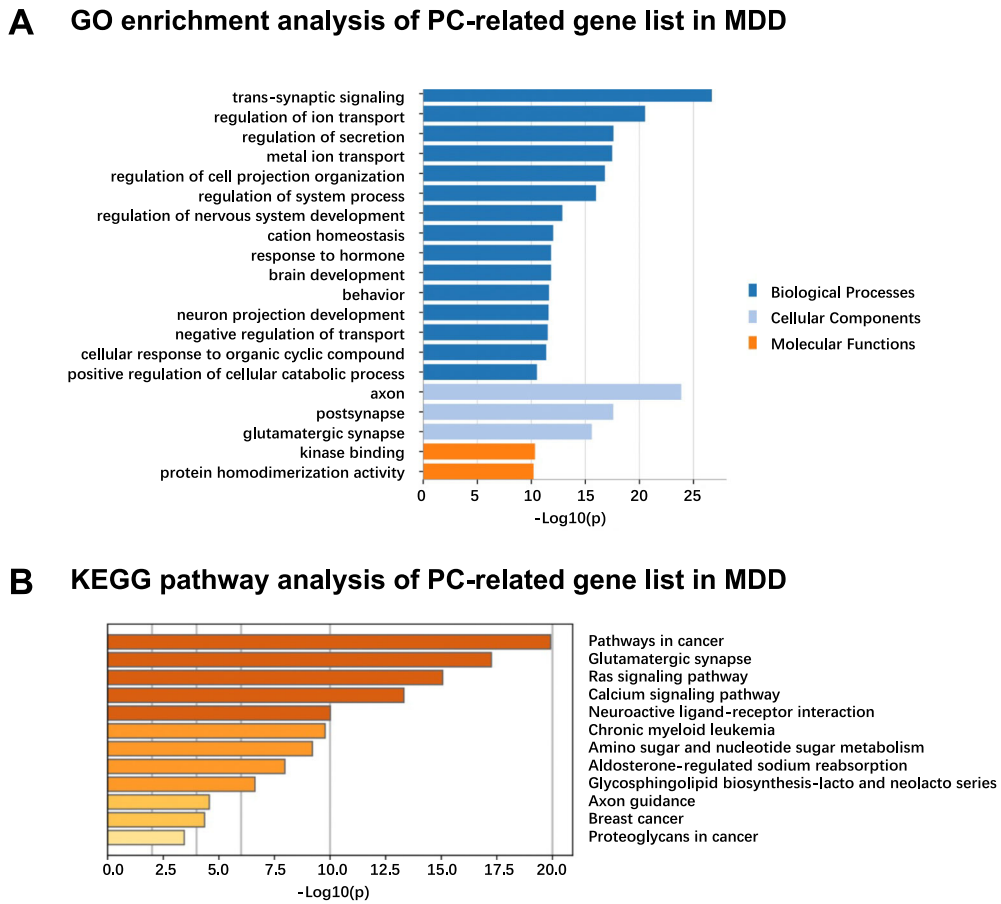

Fig. 4 GO enrichment and KEGG pathway analysis of PC-related gene list in MDD. A GO enrichment analysis of PC-related gene list in MDD.GO enrichment analysis of the list of genes with significant contribution to PC abnormal pattern related PLS1 in MDD (FDR correction, all $q < 0.01$). **B** KEGG pathway analysis of PC-related gene list in MDD. KEGG pathway analysis of PC abnormal pattern related PLS1 contribution significant gene list of MDD (FDR correction, all $q < 0.01$).

Wide modular integration of VIS-high order networks (DMN, FPN and VAN): The DMN is intricately linked with self-referential and stimulus-independent processing, while the FPN and VAN primarily handle external stimuli [44, 65]. We found wide modular integration of VIS-high order networks (DMN, FPN and VAN) in MDD patients. These interconnections between the VIS and heteromodal association cortices may lead to maladaptive integration between top-down sensory input and bottom-up regulation, affecting the selection of relevant information for goal-oriented tasks [66–68]. Thus, higher FC between VIS and higher-order networks can lead to over-integration of sensory input and regulation in MDD. Correlation analysis show that the FCs between hyper-integrated VIS nodes (left V2, right V1, and right V3) and key DMN nodes (bilateral orbital frontal cortex, right area 10 d cortex, and bilateral area dorsal 23 a + b) positively correlated with the severity of depressive symptoms. A previous study demonstrated that FC patterns between visual and frontal cortices could distinguish individuals with depression from HCs [69]. These observations suggest that alterations in VIS-higher-order networks FC could serve as biomarkers or targets for therapeutic interventions.

High integration of VIS-Limbic: The Limbic system processes sensory inputs from both internal and external environments, playing a pivotal role in diagnosis, regulation, and prediction of treatment responses in MDD [70, 71]. Recent research suggests that an entorhinal-visual cortical circuit may regulates depression-like behaviors, providing a promising target for stimulation therapy [70].Our study revealed a strong VIS-Limbic integration, which could contribute to abnormal processing of visually presented stimuli, potentially leading to negative emotional and cognitive biases in MDD [72].

Low integration of intra-VIS and VIS-SMN: We observed decreased intra-VIS FCs in MDD patients, indicating reduced internal integration within VIS, consistent with previous findings [73]. Decreased intra-VIS FCs at both region-to-module and region-to-region levels of shows significant negative correlations with depressive symptoms, while FCs of V2-ProS/VMV in the VIS positively correlated with Category Fluency of MCCB. Previous research by our team showed reduced regional homogeneity (ReHo) in the visual cortex in MDD patients, which was linked to depressive symptoms [57]. Other studies have found diminished spatial suppression during visual motion processing tasks in MDD, suggesting reduced spatial suppression as a potential endophenotype [58]. The visual cortex, a crucial component for face recognition and social communication, mediates the visual analysis of faces [74]. Our finding at both regional and module levels revealed internal reorganization and differentiation within the VIS in MDD, uncovering that these alterations are linked to depressive symptoms and processing speed. Previous research has shown reduced gamma-aminobutyric acid (GABA) levels in the occipital lobe of MDD patients, linked to depressive symptom severity [75]. It is speculated that the VIS integration disorders in MDD may be related to abnormal GABAergic interneuron gene expression. Similarly, we also identified decreased FC between the VIS and SMN, indicating disrupted multisensory integration between primary networks in MDD [76, 77].

MDD-related visual network high nodal integration and gene expression profiles

Utilizing the AHBA and employing PLS regression analysis, our connectome-transcriptome association analysis revealed that the high nodal integration observed in the MDD-related VIS is correlated with gene expression profiles enriched in pathways involved in transsynaptic signaling and ion transport regulation. Transsynaptic signaling is a fundamental biological process that supports critical molecular functions, including synapse formation and modulation of synaptic plasticity [78]. Disruptions in transsynaptic signaling can impair synapse formation and stability, significantly influencing the pathophysiology of depression [79]. Transcriptomic studies in animal models have shown that chronic stress can disrupt the brain-derived neurotrophic factor (BDNF)-tropomyosin receptor kinase B (TrkB) signaling pathway, thereby reducing ERK and Akt signaling in the hippocampus and prefrontal cortex [80, 81]. Such disruptions may decrease BDNF expression and function, leading to neuronal atrophy in areas linked to depression [80, 82, 83]. In addition to transsynaptic signaling, our analysis also revealed that genes associated with the high nodal integration in the VIS of MDD patients are enriched in pathways related to ion transport regulation. Research by Richardi and colleagues identified a significant correlation between gene enrichment for ion transport-related molecular functions and functional connectivity in the brain's resting-state network, particularly sodium ion channels and receptors, which are significantly associated with the onset of MDD [35]. Beyond the biological implications, the clinical relevance of specific high-weighted genes, such as SLC38A2 and SCN1B, is also noteworthy. SLC38A2 encodes a sodium-dependent amino acid transporter that regulates glutamine transmembrane transport, influencing synaptic activity [84, 85]. Animal studies have shown that SLC38A2 is involved in the biological pathways related to depression and plays a potential role in the molecular mechanisms of depression, influencing mood regulation and neurogenesis in MDD [86]. The SCN1B encodes the β subunit of sodium channels, which controls the generation and propagation of neural signals by modulating sodium ion channels, thereby regulating neuronal excitability [87]. Similar to our findings, A's study also discovered that SCN1B, along with other genes, is associated with brain connectivity changes observed in MDD patients and found that they are involved in the sex-specific modulation of depression-related circuits [88].

The PLS1 gene, linked to the high nodal integration of the VIS in MDD, is involved in key KEGG pathways including "Pathways in Cancer," "Glutamatergic Synapse," and the "Ras Signaling Pathway," with the latter two being closely linked to MDD pathogenesis. Multiple studies have shown reduced levels of brain glutamate and glutamine in individuals with MDD, particularly in areas like the dorsolateral prefrontal cortex (DLPFC), hippocampus [89], and posterior cingulate cortex [75]. Moreover, reduced GABA levels in the posterior cingulate cortex of MDD patients are linked to visual cognitive deficits [75, 90]. Dysregulation of Ras-related genes results in impairments in the serotonin and dopamine systems, contributing to the onset of depression. As significant downstream pathways of neurotrophic factor receptors, Ras-related signaling plays a key role in synaptic plasticity. Denayer et al. reported that overactivation of the Ras-ERK pathway can lead to reduced synaptic plasticity in mice, impairing hippocampal learning and memory behaviors [91]. Notably, among the KEGG enrichment pathways associated with genes related to high nodal integration in the VIS of MDD, the "Pathways in Cancer" ranked highest in terms of gene count and significance. The concept of comorbidity between cancer and depression was previously proposed by Walker et al. in The Lancet, which found a higher rate of depression among cancer patients compared to the general population [92]. From a transcriptomic perspective, our findings suggest potentially shared or similar molecular mechanisms between MDD and cancer, providing a transcriptomic basis for the comorbidity of these two conditions. Further exploration of these functional genetic variations and related genes is expected to aid in unraveling the pathogenesis of depression, potentially offering new therapeutic targets for both depression and cancer.

In the connectome-transcriptome association analysis of abnormal VIS FCs patterns (Fig. S2), we found that the genes associated with the abnormal VIS FCs in MDD patients were highly consistent with those associated with changes in the PC in MDD. Additionally, gene weight also showed a high degree of similarity. Biological pathway analysis revealed that these abnormal connectivity patterns in the brain's functional network are significantly correlated with gene expression profiles related to synaptic transmission, transsynaptic signaling, ion transport, and other biological processes. Our main findings were confirmed through analysis of male-specific gene data and left hemisphere gene data, and the results were found to be stable and reliable, further elucidating the molecular basis of large-scale functional network abnormalities in MDD patients under resting state. This provides new imaging-transcriptomic evidence for the role of synaptic and ion transport-related pathways in the pathophysiology of depression.

Limitation

The study's sample included individuals taking medication and lacked longitudinal data on treatment responses. While the study identified increased connectivity changes in the visual network among MDD patients, its specificity across different MDD subtypes remains unclear. The analysis, while informative, fell short in fully elucidating the underlying pathogenesis, calling for a more comprehensive approach involving transcriptomics. Additionally, the gene expression data used, derived from the AIBS and based on non-Chinese populations, may affect the results due to potential ethnic differences in gene expression profiles. This underscores the need for larger, more diverse datasets from MDD patients for further validation. Furthermore, the study primarily reports associations rather than causal relationships, high lighting the need for further research on the interplay between genes and the brain in the context of the disease phenotype.

CONCLUSION

In this investigation, we established a comprehensive analysis to explore the connection between MDD-related connectome dysfunctions and gene expression patterns. Our findings revealed a significant correlation between the atypical connectivity patterns within the brain's functional network system in MDD patients and the gene expression profiles related to synaptic and trans-synaptic transmission, ion transport, and other crucial biological processes. This correlation sheds light on the molecular biological underpinnings of the anomalies observed in the large-scale functional network systems of individuals with MDD. The implications of these findings are substantial, paving the way for the development of more targeted and effective treatment modalities in the future, thereby enhancing the clinical management and therapeutic outcomes for individuals grappling with MDD.

DATA AVAILABILITY

Human gene expression data that support the findings of this study are available in the Allen Brain Atlas ("Complete normalized microarray datasets", https://human.brainmap.org/static/download). The probe-to-gene annotations were obtained by the Re-annotator toolkit (v1.0.0, https://sourceforge.net/projects/reannotator/). The data that support the findings of this study are available from the corresponding author through request.

REFERENCES

1. Malhi GS, Mann JJ. Depression. Lancet. 2018;392:2299–312.
2. Kruijshaar ME, Barendregt J, Vos T, de Graaf R, Spijker J, Andrews G. Lifetime prevalence estimates of major depression: an indirect estimation method and a quantification of recall bias. Eur J Epidemiol. 2005;20:103–11.
3. Spellman T, Liston C. Toward circuit mechanisms of pathophysiology in depression. Am J Psychiatry. 2020;177:381–90.
4. Mulders PC, van Eijndhoven PF, Schene AH, Beckmann CF, Tendolkar I. Resting-state functional connectivity in major depressive disorder: a review. Neurosci Biobehav Rev. 2015;56:330–44.
5. Bertolero MA, Yeo BTT, D'Esposito M. The modular and integrative functional architecture of the human brain. Proc Natl Acad Sci USA. 2015;112:E6798–E807.
6. Gong Q, He Y. Depression, neuroimaging and connectomics: a selective overview. Biol Psychiatry. 2015;77:223–35.
7. Gong Q, Hu X, Pettersson-Yeo W, Xu X, Lui S, Crossley N, et al. Network-level dysconnectivity in drug-naïve first-episode psychosis: dissociating transdiagnostic and diagnosis-specific alterations. Neuropsychopharmacology. 2017;42:933–40.
8. Sporns O, Betzel RF. Modular brain networks. Annu Rev Psychol. 2016;67:613–40.
9. Marek S, Hwang K, Foran W, Hallquist MN, Luna B. The contribution of network organization and integration to the development of cognitive control. PLoS Biol. 2015;13:e1002328.
10. He Y, Wang J, Wang L, Chen ZJ, Yan C, Yang H, et al. Uncovering intrinsic modular organization of spontaneous brain activity in humans. PLoS ONE. 2009;4:e5226.
11. Sendi MSE, Zendehrouh E, Sui J, Fu Z, Zhi D, Lv L, et al. Abnormal dynamic functional network connectivity estimated from default mode network predicts symptom severity in major depressive disorder. Brain Connect. 2021;11:838–49.
12. Yan CG, Chen X, Li L, Castellanos FX, Bai TJ, Bo QJ, et al. Reduced default mode network functional connectivity in patients with recurrent major depressive disorder. Proc Natl Acad Sci USA. 2019;116:9078–83.
13. Zhu X, Zhu Q, Shen H, Liao W, Yuan F. Rumination and default mode network subsystems connectivity in first-episode, drug-naive young patients with major depressive disorder. Sci Rep. 2017;7:43105.
14. Lan Z, Zhang W, Wang D, Tan Z, Wang Y, Pan C, et al. Decreased modular segregation of the frontal-parietal network in major depressive disorder. Front Psychiatry. 2022;13:929812.
15. Pan F, Xu Y, Zhou W, Chen J, Wei N, Lu S, et al. Disrupted intrinsic functional connectivity of the cognitive control network underlies disease severity and executive dysfunction in first-episode, treatment-naive adolescent depression. J Affect Disord. 2020;264:455–63.
16. He Y, Lim S, Fortunato S, Sporns O, Zhang L, Qiu J, et al. Reconfiguration of cortical networks in MDD uncovered by multiscale community detection with fMRI. Cerebral Cortex (New York, NY: 1991). 2018;28:1383–95.
17. Sun X, Sun J, Lu X, Dong Q, Zhang L, Wang W, et al. Mapping neurophysiological subtypes of major depressive disorder using normative models of the functional connectome. Biol Psychiatry. 2023;94:936–47.
18. Godfrey KEM, Muthukumaraswamy SD, Stinear CM, Hoeh N. Decreased salience network fMRI functional connectivity following a course of rTMS for treatment-resistant depression. J Affect Disord. 2022;300:235–42.
19. Sikora M, Heffernan J, Avery ET, Mickey BJ, Zubieta J-K, Peciña M. Salience network functional connectivity predicts placebo effects in major depression. Biol Psychiatry Cogn Neurosci Neuroimaging. 2016;1:68–76.
20. Beevers CG, Clasen PC, Enock PM, Schnyer DM. Attention bias modification for major depressive disorder: effects on attention bias, resting state connectivity, and symptom change. J Abnorm Psychol. 2015;124:463–75.
21. Rayner G, Jackson G, Wilson S. Cognition-related brain networks underpin the symptoms of unipolar depression: evidence from a systematic review. Neurosci Biobehav Rev. 2016;61:53–65.
22. Disner SG, Beevers CG, Haigh EAP, Beck AT. Neural mechanisms of the cognitive model of depression. Nat Rev Neurosci. 2011;12:467–77.
23. Lu F, Cui Q, Huang X, Li L, Duan X, Chen H, et al. Anomalous intrinsic connectivity within and between visual and auditory networks in major depressive disorder. Prog Neuropsychopharmacol Biol Psychiatry. 2020;100:109889.
24. Guo W-B, Liu F, Xue Z-M, Xu X-J, Wu R-R, Ma C-Q, et al. Alterations of the amplitude of low-frequency fluctuations in treatment-resistant and treatment-response depression: a resting-state fMRI study. Prog Neuropsychopharmacol Biol Psychiatry. 2012;37:153–60.
25. Gallo S, El-Gazzar A, Zhutovsky P, Thomas RM, Javaheripour N, Li M, et al. Functional connectivity signatures of major depressive disorder: machine learning analysis of two multicenter neuroimaging studies. Mol Psychiatry. 2023;28:3013–22.
26. Peng D, Shi F, Shen T, Peng Z, Zhang C, Liu X, et al. Altered brain network modules induce helplessness in major depressive disorder. J Affect Disord. 2014;168:21–9.
27. Flint J, Kendler KS. The genetics of major depression. Neuron. 2014;81:1214.
28. McIntosh AM, Sullivan PF, Lewis CM. Uncovering the genetic architecture of major depression. Neuron. 2019;102:91–103.
29. Mullins N, Lewis CM. Genetics of depression: progress at last. Curr Psychiatry Rep. 2017;19:43.
30. Zheng J, Womer FY, Tang L, Guo H, Zhang X, Tang Y, et al. Integrative omics analysis reveals epigenomic and transcriptomic signatures underlying brain structural deficits in major depressive disorder. Transl Psychiatry. 2024;14:17.
31. Wray NR, Ripke S, Mattheisen M, Trzaskowski M, Byrne EM, Abdellaoui A, et al. Genome-wide association analyses identify 44 risk variants and refine the genetic architecture of major depression. Nat Genet. 2018;50:668–81.
32. Xia M, Liu J, Mechelli A, Sun X, Ma Q, Wang X, et al. Connectome gradient dysfunction in major depression and its association with gene expression profiles and treatment outcomes. Mol Psychiatry. 2022;27:1384–93.
33. Hibar DP, Stein JL, Renteria ME, Arias-Vasquez A, Desrivières S, Jahanshad N, et al. Common genetic variants influence human subcortical brain structures. Nature. 2015;520:224–9.
34. Hawrylycz MJ, Lein ES, Guillozet-Bongaarts AL, Shen EH, Ng L, Miller JA, et al. An anatomically comprehensive atlas of the adult human brain transcriptome. Nature. 2012;489:391–9.
35. Richiardi J, Altmann A, Milazzo AC, Chang C, Chakravarty MM, Banaschewski T, et al. BRAIN NETWORKS. Correlated gene expression supports synchronous activity in brain networks. Science. 2015;348:1241–4.
36. Fornito A, Arnatkeviciute A, Fulcher BD. Bridging the gap between connectome and transcriptome. Trends Cogn Sci. 2019;23:34–50.
37. Liu J, Xia M, Wang X, Liao X, He Y. The spatial organization of the chronnectome associates with cortical hierarchy and transcriptional profiles in the human brain. Neuroimage. 2020;222:117296.
38. Vertes PE, Rittman T, Whitaker KJ, Romero-Garcia R, Vasa F, Kitzbichler MG, et al. Gene transcription profiles associated with inter-modular hubs and connection distance in human functional magnetic resonance imaging networks. Philos Trans R Soc Lond B Biol Sci. 2016;371:20150362.
39. Hawrylycz M, Miller JA, Menon V, Feng D, Dolbeare T, Guillozet-Bongaarts AL, et al. Canonical genetic signatures of the adult human brain. Nat Neurosci. 2015;18:1832–44.
40. Wang J, Wang X, Xia M, Liao X, Evans A, He Y. GRETNA: a graph theoretical network analysis toolbox for imaging connectomics. Front Hum Neurosci. 2015;9:386.
41. Glasser MF, Coalson TS, Robinson EC, Hacker CD, Harwell J, Yacoub E, et al. A multi-modal parcellation of human cerebral cortex. Nature. 2016;536:171–8.
42. Achard S, Bullmore E. Efficiency and cost of economical brain functional networks. PLoS Comput Biol. 2007;3:e17.
43. Yin P, Zhao C, Li Y, Liu X, Chen L, Hong N. Changes in brain structure, function, and network properties in patients with first-episode schizophrenia treated with antipsychotics. Front Psychiatry. 2021;12:735623.
44. Yeo BTT, Krienen FM, Sepulcre J, Sabuncu MR, Lashkari D, Hollinshead M, et al. The organization of the human cerebral cortex estimated by intrinsic functional connectivity. J Neurophysiol. 2011;106:1125–65.
45. Du H, Xia M, Zhao K, Liao X, Yang H, Wang Y, et al. PAGANI toolkit: parallel graph-theoretical analysis package for brain network big data. Hum Brain Mapp. 2018;39:1869–85.
46. Hwang K, Hallquist MN, Luna B. The development of hub architecture in the human functional brain network. Cereb Cortex. 2013;23:2380–93.
47. Power JD, Schlaggar BL, Lessov-Schlaggar CN, Petersen SE. Evidence for hubs in human functional brain networks. Neuron. 2013;79:798–813.
48. Arnatkeviciute A, Fulcher BD, Fornito A. A practical guide to linking brain-wide gene expression and neuroimaging data. Neuroimage. 2019;189:353–67.
49. Abdi H. Partial least squares regression and projection on latent structure regression (PLS Regression). Wiley Interdiscip. Rev. Comput. Stat. 2010;2:97–106.
50. Whitaker KJ, Vertes PE, Romero-Garcia R, Vasa F, Moutoussis M, Prabhu G, et al. Adolescence is associated with genomically patterned consolidation of the hubs of the human brain connectome. Proc Natl Acad Sci USA. 2016;113:9105–10.
51. Zhou Y, Zhou B, Pache L, Chang M, Khodabakhshi AH, Tanaseichuk O, et al. Metascape provides a biologist-oriented resource for the analysis of systems-level datasets. Nat Commun. 2019;10:1523.
52. Li J, Seidlitz J, Suckling J, Fan F, Ji G-J, Meng Y, et al. Cortical structural differences in major depressive disorder correlate with cell type-specific transcriptional signatures. Nat Commun. 2021;12:1647.
53. Wandell BA, Dumoulin SO, Brewer AA. Visual field maps in human cortex. Neuron. 2007;56:366–83.
54. Vetter P, Smith FW, Muckli L. Decoding sound and imagery content in early visual cortex. Curr Biol. 2014;24:1256–62.
55. Chen H, Liu K, Zhang B, Zhang J, Xue X, Lin Y, et al. More optimal but less regulated dorsal and ventral visual networks in patients with major depressive disorder. J Psychiatr Res. 2019;110:172–8.

56. Ancelin M-L, Carrière I, Artero S, Maller J, Meslin C, Ritchie K, et al. Lifetime major depression and grey-matter volume. J Psychiatry Neurosci. 2019;44:45–53.
57. Wei Y-G, Duan J, Womer FY, Zhu Y, Yin Z, Cui L, et al. Applying dimensional psychopathology: transdiagnostic associations among regional homogeneity, leptin and depressive symptoms. Transl Psychiatry. 2020;10:248.
58. Golomb JD, McDavitt JRB, Ruf BM, Chen JI, Saricicek A, Maloney KH, et al. Enhanced visual motion perception in major depressive disorder. J Neurosci. 2009;29:9072–7.
59. Suh JS, Schneider MA, Minuzzi L, MacQueen GM, Strother SC, Kennedy SH, et al. Cortical thickness in major depressive disorder: a systematic review and meta-analysis. Prog Neuropsychopharmacol Biol Psychiatry. 2019;88:287–302.
60. Lee JS, Kang W, Kang Y, Kim A, Han K-M, Tae W-S, et al. Alterations in the occipital cortex of drug-naïve adults with major depressive disorder: a surface-based analysis of surface area and cortical thickness. Psychiatry Investig. 2021;18:1025–33.
61. Gong J, Wang J, Qiu S, Chen P, Luo Z, Wang J, et al. Common and distinct patterns of intrinsic brain activity alterations in major depression and bipolar disorder: voxel-based meta-analysis. Transl Psychiatry. 2020;10:353.
62. de Kwaasteniet BP, Rive MM, Ruhé HG, Schene AH, Veltman DJ, Fellinger L, et al. Decreased resting-state connectivity between neurocognitive networks in treatment resistant depression. Front Psychiatry. 2015;6:28.
63. He Z, Cui Q, Zheng J, Duan X, Pang Y, Gao Q, et al. Frequency-specific alterations in functional connectivity in treatment-resistant and -sensitive major depressive disorder. J Psychiatr Res. 2016;82:30–9.
64. Guo W, Liu F, Xue Z, Gao K, Liu Z, Xiao C, et al. Decreased interhemispheric coordination in treatment-resistant depression: a resting-state fMRI study. PLoS ONE. 2013;8:e71368.
65. Smallwood J, Bernhardt BC, Leech R, Bzdok D, Jefferies E, Margulies DS. The default mode network in cognition: a topographical perspective. Nat Rev Neurosci. 2021;22:503–13.
66. Chadick JZ, Gazzaley A. Differential coupling of visual cortex with default or frontal-parietal network based on goals. Nat Neurosci. 2011;14:830–2.
67. Lerman-Sinkoff DB, Sui J, Rachakonda S, Kandala S, Calhoun VD, Barch DM. Multimodal neural correlates of cognitive control in the human connectome project. Neuroimage. 2017;163:41–54.
68. Zhang H, Meng C, Di X, Wu X, Biswal B. Static and dynamic functional connectome reveals reconfiguration profiles of whole-brain network across cognitive states. Netw Neurosci. 2023;7:1034–50.
69. Le TM, Borghi JA, Kujawa AJ, Klein DN, Leung H-C. Alterations in visual cortical activation and connectivity with prefrontal cortex during working memory updating in major depressive disorder. Neuroimage Clin. 2017;14:43–53.
70. Lu J, Zhang Z, Yin X, Tang Y, Ji R, Chen H, et al. An entorhinal-visual cortical circuit regulates depression-like behaviors. Mol Psychiatry. 2022;27:3807–20.
71. Lai C-H. Fronto-limbic neuroimaging biomarkers for diagnosis and prediction of treatment responses in major depressive disorder. Prog Neuropsychopharmacol Biol Psychiatry. 2021;107:110234.
72. Fusar-Poli P, Placentino A, Carletti F, Landi P, Allen P, Surguladze S, et al. Functional atlas of emotional faces processing: a voxel-based meta-analysis of 105 functional magnetic resonance imaging studies. J Psychiatry Neurosci. 2009;34:418–32.
73. Ma Q, Tang Y, Wang F, Liao X, Jiang X, Wei S, et al. Transdiagnostic dysfunctions in brain modules across patients with schizophrenia, bipolar disorder, and major depressive disorder: a Connectome-Based Study. Schizophr Bull. 2020;46:699–712.
74. Haxby JV, Hoffman EA, Gobbini MI. Human neural systems for face recognition and social communication. Biol Psychiatry. 2002;51:59–67.
75. Song XM, Hu X-W, Li Z, Gao Y, Ju X, Liu D-Y, et al. Reduction of higher-order occipital GABA and impaired visual perception in acute major depressive disorder. Mol Psychiatry. 2021;26:6747–55.
76. Lewkowicz DJ, Ghazanfar AA. The emergence of multisensory systems through perceptual narrowing. Trends Cogn Sci. 2009;13:470–8.
77. Tang X, Wu J, Shen Y. The interactions of multisensory integration with endogenous and exogenous attention. Neurosci Biobehav Rev. 2016;61:208–24.
78. de Wit J, Ghosh A. Specification of synaptic connectivity by cell surface interactions. Nat Rev Neurosci. 2016;17:22–35.
79. Duman RS, Voleti B. Signaling pathways underlying the pathophysiology and treatment of depression: novel mechanisms for rapid-acting agents. Trends Neurosci. 2012;35:47–56.
80. Kang HJ, Voleti B, Hajszan T, Rajkowska G, Stockmeier CA, Licznerski P, et al. Decreased expression of synapse-related genes and loss of synapses in major depressive disorder. Nat Med. 2012;18:1413–7.
81. Duman RS, Aghajanian GK. Synaptic dysfunction in depression: potential therapeutic targets. Science. 2012;338:68–72.
82. Duman RS, Li N, Liu R-J, Duric V, Aghajanian G. Signaling pathways underlying the rapid antidepressant actions of ketamine. Neuropharmacology. 2012;62:35–41.
83. Feyissa AM, Chandran A, Stockmeier CA, Karolewicz B. Reduced levels of NR2A and NR2B subunits of NMDA receptor and PSD-95 in the prefrontal cortex in major depression. Prog Neuropsychopharmacol Biol Psychiatry. 2009;33:70–5.
84. Shimamoto A, Rappeneau V, Munjal H, Farris T, Davis C, Wilson A, et al. Glutamate-glutamine transfer and chronic stress-induced sex differences in cocaine responses. Neuroscience. 2018;391:104–19.
85. Salemi M, Ravo M, Lanza G, Schillaci FA, Ventola GM, Marchese G, et al. Gene expression profiling of post mortem midbrain of Parkinson's disease patients and healthy controls. Int J Mol Sci. 2024;25:707.
86. Malki K, Tosto MG, Mouriño-Talín H, Rodríguez-Lorenzo S, Pain O, Jumhaboy I, et al. Highly polygenic architecture of antidepressant treatment response: comparative analysis of SSRI and NRI treatment in an animal model of depression. Am J Med Genet B Neuropsychiatr Genet. 2017;174:235–50.
87. Chancey JH, Ahmed AA, Guillén FI, Ghatpande V, Howard MA. Complex synaptic and intrinsic interactions disrupt input/output functions in the hippocampus of Scn1b Knock-Out mice. J Neurosci. 2023;43:8562–77.
88. Talishinsky A, Downar J, Vértes PE, Seidlitz J, Dunlop K, Lynch CJ, et al. Regional gene expression signatures are associated with sex-specific functional connectivity changes in depression. Nat Commun. 2022;13:5692.
89. Duman RS, Sanacora G, Krystal JH. Altered connectivity in depression: GABA and glutamate neurotransmitter deficits and reversal by novel treatments. Neuron. 2019;102:75–90.
90. Prévot T, Sibille E. Altered GABA-mediated information processing and cognitive dysfunctions in depression and other brain disorders. Mol Psychiatry. 2021;26:151–67.
91. Denayer E, Ahmed T, Brems H, Van Woerden G, Borgesius NZ, Callaerts-Vegh Z, et al. Spred1 is required for synaptic plasticity and hippocampus-dependent learning. J Neurosci. 2008;28:14443–9.
92. Walker J, Hansen CH, Martin P, Symeonides S, Ramessur R, Murray G, et al. Prevalence, associations, and adequacy of treatment of major depression in patients with cancer: a cross-sectional analysis of routinely collected clinical data. Lancet Psychiatry. 2014;1:343–50.
93. Xia M, Wang J, He Y. BrainNet viewer: a network visualization tool for human brain connectomics. PLoS ONE. 2013;8:e68910.

ACKNOWLEDGEMENTS

This study was funded by National Science Fund for Distinguished Young Scholars (81725005 to Fei Wang), Liaoning Education Foundation (Pandeng Scholar to Fei Wang), National Natural Science Foundation of China (82071998 and 82021004 to Mingrui Xia), Beijing Natural Science Foundation (JQ23033 to Mingrui Xia, and Liaoning Joint Fund Project Doctoral Research Launch Project (2023-BSBA-192 to Mingrui Zhu).

AUTHOR CONTRIBUTIONS

Authors Mingrui Zhu, Yifan Chen, Junjie Zheng, Pengfei Zhao, Mingrui Xia, Yanqing Tang, Fei Wang were involved in participants recruitment and data collection. Mingrui Zhu, Mingrui Xia executed the neuroimaging and omics data analysis. Mingrui Zhu, Yifan Chen and Fei Wang wrote the first draft of the manuscript. Mingrui Xia, Yanqing Tang and Fei Wang guided the study design. Fei Wang supervised the whole study and revised the manuscript. All of the authors contributed to the final version of the paper.

COMPETING INTERESTS

The authors declare no competing interests.

ETHICS STATEMENT

All methods were performed in accordance with the relevant guidelines and regulations.

ADDITIONAL INFORMATION

Supplementary information The online version contains supplementary material available at https://doi.org/10.1038/s41398-025-03265-y.

Correspondence and requests for materials should be addressed to Mingrui Xia, Yanqing Tang or Fei Wang.